Elimination of intracellular Ca^{2+} overload by BAPTA-AM liposome nanoparticles: A promising treatment for acute pancreatitis

ZAILIN FU[1,2], DINGSHENG WANG[1], CAIYUN ZHENG[2], MINGHUA XIE[1], YIFANG CHEN[1], YI ZHOU[1], YAN HUANG[1], YING SONG[2] and WEIYONG HONG[3]

[1]Department of Pharmacy, Linping Branch, The Second Affiliated Hospital, Zhejiang University School of Medicine; [2]Department of Pharmacology, College of Pharmaceutical Sciences, Zhejiang University of Technology, Hangzhou, Zhejiang 310000; [3]Department of Pharmacy, Municipal Hospital Affiliated to Taizhou University, Taizhou, Zhejiang 318000, P.R. China

Received August 1, 2023; Accepted January 18, 2024

DOI: 10.3892/ijmm.2024.5358

Abstract. Calcium overload, a notable instigator of acute pancreatitis (AP), induces oxidative stress and an inflammatory cascade, subsequently activating both endogenous and exogenous apoptotic pathways. However, there is currently lack of available pharmaceutical interventions to alleviate AP by addressing calcium overload. In the present study, the potential clinical application of liposome nanoparticles (LNs) loaded with 1,2-bis(2-aminophenoxy)ethane-N,N,N',N'-tetraacetic acid tetrakis (acetoxymethyl ester) (BAPTA-AM), a cell-permeant calcium chelator, was investigated as a therapeutic approach for the management of AP. To establish the experimental models *in vitro*, AR42J cells were exposed to high glucose/sodium oleate (HGO) to induce necrosis, and *in vivo*, intra-ductal taurocholate (TC) infusion was used to induce AP. The findings of the present study indicated that the use of BAPTA-AM-loaded LN (BLN) effectively and rapidly eliminated excessive Ca^{2+} and reactive oxygen species, suppressed mononuclear macrophage activation and the release of inflammatory cytokines, and mitigated pancreatic acinar cell apoptosis and necrosis induced by HGO. Furthermore, the systemic administration of BLN demonstrated promising therapeutic potential in the rat model of AP. Notably, BLN significantly enhanced the survival rates of rats subjected to the TC challenge, increasing from 37.5 to 75%. This improvement was attributed to the restoration of pancreatic function, as indicated by improved blood biochemistry indices and alleviation of pancreatic lesions. The potential therapeutic efficacy of BLN in rescuing patients with AP is likely attributed to its capacity to inhibit oxidative stress, prevent premature activation of zymogens and downregulate the expression of TNF-α, IL-6 and cathepsin B. Thus, BLN demonstrated promising value as a novel therapeutic approach for promptly alleviating the burden of intracellular Ca^{2+} overload in patients with AP.

Correspondence to: Professor Ying Song, Department of Pharmacology, College of Pharmaceutical Sciences, Zhejiang University of Technology, 18 Chaowang Road, Hangzhou, Zhejiang 310000, P.R. China
E-mail: songying@zjut.edu.cn

Dr Weiyong Hong, Department of Pharmacy, Municipal Hospital Affiliated to Taizhou University, 381 East Zhongshan Road, Taizhou, Zhejiang 318000, P.R. China
E-mail: weiyongh@126.com

Key words: BAPTA-AM, liposome nanoparticles, calcium overload, acute pancreatitis, anti-apoptosis, anti-necrosis

Introduction

Acute pancreatitis (AP) is a widely observed and severe clinical condition characterised by the abnormal activation of enzymes within the pancreas, leading to a series of inflammatory responses including autodigestion, edema, hemorrhage and potentially necrosis (1-3). Despite advancements in our understanding of the pathogenesis of AP pathogenesis, the prevalence of the disease continues to increase each year, with ~20% of patients progressing to severe AP (SAP). SAP can subsequently evolve into a systemic inflammatory response and a multiple organ dysfunction syndrome, ultimately resulting in considerably high mortality rates with a range of 20-40% (4-7). At present, the primary emphasis in the management of AP is on providing supportive care, including fluid resuscitation, pain management and parenteral nutrition support (4,8,9). The etiologies underlying the development and progression of AP are complex, encompassing various apoptotic and necrotic signaling pathways. Nevertheless, the therapeutic options for targeting the underlying causes are severely limited. The currently available medications, such as somatostatin and gabexate, solely serve to inhibit excessive pancreatic enzyme activity, without effectively intercepting the premature activation of zymogens, oxidative stress-induced injuries and inflammatory responses during the course of AP (10,11). AP is characterised by the abrupt and extensive destruction of pancreatic acinar cells, encompassing

various apoptotic signaling pathways. Merely targeting a single pathway is insufficient for effectively treating patients with AP, particularly those with SAP.

The accumulation of Ca^{2+} within pancreatic acinar cells plays a pivotal role in the pathological progression of AP (12). Various conditions, including biliary tract obstruction, hyperlipidemia, hyperparathyroidism, alcoholism and abdominal infection among others, can facilitate the influx and release of Ca^{2+} from the endoplasmic reticulum, leading to subsequent Ca^{2+}-related consequences (13-15). The shared mechanism among the aforementioned diseases involves excessive accumulation of cytoplasmic Ca^{2+}, which subsequently triggers the activation of Ca^{2+}-dependent proteases and lipases. These enzymes then proceed to hydrolyze the cytoskeleton, leading to cellular collapse and compromised membrane integrity (16). Consequently, this exacerbates Ca^{2+} overload, ultimately amplifying cell death (17,18). Additionally, the sustained Ca^{2+} overload in the mitochondria can induce excessive production of reactive oxygen species (ROS), resulting in lipid peroxidation of cell membranes which further enhances the permeability of the cell membranes and exacerbates the Ca^{2+} overload. The interplay between Ca^{2+} overload and ROS results in a reciprocal reinforcement, leading to a cascading feedback loop that ultimately culminates in cellular collapse. Additionally, the occurrence of Ca^{2+} overload at an early stage in the process of apoptosis and necrosis stimulates the expression and release of proinflammatory cytokines, such as TNF-α and IL-6, by inflammatory cells. It is worth noting that TNF-α not only initiates inflammatory signaling pathways but also facilitates exogenous cell apoptosis through its binding to TNF-receptor 1 (TNF-R1). The activation of TNF-R1 triggers premature zymogen activation and excessive secretion of cathepsin B, further exacerbating the cellular response (19,20). The excessive production and activation of zymogens exacerbate the autodigestion of pancreatic acinar cells. The increased levels of cathepsin B also contribute to apoptosis, pyroptosis, ferroptosis, necroptosis and autophagic cell death (21). Specifically, an overload of cytoplasmic Ca^{2+} prompts the fusion of lysosomes and zymogen granules, which is essential for the aforementioned pathological processes (20,22,23). Therefore, the fluctuation of intracellular Ca^{2+} $[Ca^{2+}]i$ plays a crucial role in the regulation of TNF-α/cathepsin B-mediated necroptotic and apoptotic signaling pathways, as well as the modulation of inflammatory responses (23-26). Moreover, an excessive increase in $[Ca^{2+}]i$ leads to the proliferation of ROS, which disrupts the functioning of both the cytoplasmic and mitochondrial membranes, ultimately resulting in cell apoptosis or necrosis (27,28). Therefore, promptly restoring $[Ca^{2+}]i$ levels from an overloaded state (10^{-5}-10^{-4} mol/l) to a resting state (~10^{-7} mol/l) presents a viable approach to mitigate cellular damage and rescue endangered cells.

In order to achieve this goal, 1,2-bis(2-aminophenoxy) ethane-N,N,N',N'-tetraacetic acid tetrakis (acetoxymethyl ester) (BAPTA-AM), a cell-permeant Ca^{2+} chelator, has emerged as a suitable candidate for the management of AP, as opposed to Ca^{2+} channel blockers (CCBs) (16). CCBs have limited efficacy in mitigating Ca^{2+} overload and do not impact Ca^{2+} release from intracellular stores (29). The pathogenesis of acinar cell death in AP is intricate and interconnected. Targeting a single aspect of the pathogenesis of AP is insufficient to effectively halt its progression. Calcium overload serves as a pivotal factor in this intricate pathogenic process (Fig. S1). BAPTA-AM, a compound capable of penetrating acinar cells, undergoes hydrolysis by esterase enzymes upon cellular entry, transforming into the active chelator BAPTA, which can then selectively and rapidly pair with Ca^{2+}, thus diminishing the intracellular Ca^{2+} overload (Fig. S2) (30). Nevertheless, the hydrophobic nature of BAPTA-AM poses a notable obstacle to its direct use for the preservation of endangered cells. To address this issue, liposomes, particularly nanoscale liposomes, have been employed to enhance the solubility of hydrophobic drugs, modify drug absorption, prolong biological half-life and imbue more specific targeting and biocompatible characteristics. Additionally, the lipid bilayer of liposomes serves as a protective barrier, preventing extracellular nonspecific hydrolysis of ester compounds such as BAPTA-AM. Consequently, the ability of BAPTA to chelate Ca^{2+} in the extracellular fluid is rendered ineffective. Given the advantages of liposomes and the good solubility of BAPTA-AM in lipids, BAPTA-AM liposome nanoparticles (BLNs) were prepared in the present study.

Our previous studies demonstrated the promising therapeutic potential of BAPTA-AM in mitigating ischemia reperfusion-induced acute kidney injury and D-GalN/lipopolysaccharide (LPS) induced fulminant hepatic failure through the reduction of overloaded $[Ca^{2+}]i$ (31,32). In the present study, the rescuing effects of BLN both *in vitro* and *in vivo* were assessed. The evaluation of survival rates, pancreatic function indicators and pancreas microcirculation were examined. Additionally, the impact of BLN on the pathways of pancreatic necrosis and apoptosis was performed to elucidate the underlying protective mechanism.

Materials and methods

Materials. BAPTA-AM (>95% pure), L-α-phosphatidylcholine, cholesterol, sodium oleate, sodium cholate, glucose and ulinastatin were purchased from Shanghai Aladdin Biochemical Technology Co., Ltd. Thiazolyl blue and lipopolysaccharide (LPS) were obtained from Sigma-Aldrich; Merck KGaA. Biochemical test kits used for α-amylase (AMS), triglycerides (TGs), lactate dehydrogenase (LDH), malondialdehyde (MDA) and superoxide dismutase (SOD) were obtained from the Nanjing Jiancheng Bioengineering Institute. ELISA quantification kits for TNF-α (cat. no. ek0526) and IL-6 (cat. no. ek0412) were obtained from Wuhan Boster Biological Technology, Ltd. Annexin V-FITC/PI kits, Kaighn's modified Ham's F-12 Medium (F12K), Dulbecco's modification of Eagle's medium (DMEM) and D-Hanks buffer were obtained from Procell Life Science & Technology Co., Ltd. Fetal bovine serum (FBS) was purchased from Thermo Fisher Scientific, Inc. Fura-3/AM was purchased from Shanghai Beyotime Biotech Co., Ltd. Primary antibodies against TNF-α (cat. no. ab6671), cathepsin B (cat. no. ab214428) and goat anti-rabbit IgG H&L (HRP; cat. no. ab6721) were purchased from Abcam; TRIzol® reagent was purchased from Thermo Fisher Scientific; BioRT cDNA First Strand Synthesis kit was purchased from Hangzhou Bioer Co., Ltd. and primers targeting cathepsin B, TNF-α and β-actin mRNA were synthesized by Shanghai Sangon Biotech Co., Ltd.

Preparation and characterization of BLN. BLN was prepared using a thin-film hydration method followed by an extrusion technique (31). Briefly, a mixture of 100 mg L-α-phosphatidylcholine, 5 mg BAPTA-AM, 10 mg cholesterol and 15 mg Tween 80 was dissolved in 10 ml chloroform in an eggplant flask. The chloroform was then evaporated slowly under reduced pressure at 50˚C using rotary evaporation, resulting in a uniform lipid film. Subsequently, the lipid film was hydrated by adding 10 ml PBS and agitating at 40˚C for 1 h, leading to the formation of a primary suspension. The primary suspension was further processed by extruding it through a 200-nm polycarbonate membrane for three cycles to obtain nanoscale liposomes. The mean particle size, polydispersity index (PDI) and ζ potential of BLN in a 5% glucose injection were measured using a Malvern Zetasizer NanoZS90 (Malvern Instruments Ltd.). The morphology of BLN was analyzed using scanning electron microscopy (SEM; JSM-6510LV, JEOL, Ltd.). BLN was diluted to a concentration of 0.01 mg/ml, and ~10 μl of the dilution (equivalent to ~one drop) was carefully dripped onto the substrate. Subsequently, the solution was allowed to slowly disperse and dry at room temperature under a nitrogen atmosphere in order to facilitate uniform spreading. Finally, gold coating was applied on BLN using vacuum-assisted spraying technique. SEM detection parameters included: Voltage set at 5 kV, horizontal field width of 25.4 μm, working distance maintained at 9.4 mm, SEM mode used for imaging and pressure maintained at 3.00e-6 Torr. The encapsulation efficiency of BAPTA-AM in liposome nanoparticles (LNs) was assessed using microcolumn centrifugation. Specifically, BLN was added and allowed to seep into a microcolumn containing Sephadex G-50. The entire assembly was then centrifuged at room temperature (600 x g for 3 min), with distilled water serving as the eluent. These procedures were conducted in triplicate. The unencapsulated free BAPTA-AM was separated from BLN by passing it through a microcolumn and determined with high-performance liquid chromatography (HPLC; 1260, Agilent Technologies, Inc.). The HPLC analysis was performed on a C18 Column (150x4.6 mm i.d., 3.5 μm) with a detection wavelength of 250 nm. Elution consisted of 65:35 (v/v) methanol/water with ammonium acetate (50 mmol/l) as the mobile phase initiated at a flow rate of 1 ml/min at 30˚C. The volume of each injection was 20 μl. Encapsulation efficiency (EE) was calculated using the equation: EE (%)=(BAPTA-AM$_{total}$-BAPTA-AM$_{unencapsulated}$)/(BAPTA-AM$_{total}$) x100.

Liposomes with 7.5% (w/v) trehalose as a lyoprotectant were freeze-dried on a scheduled procedure using an Alpha 1-2 LD Plus lyophilizer (Martin Christ Inc.). Size distribution and drug leakage were analyzed after reconstitution of the lyophilized BLN in PBS (pH 7.4) solution.

Cell culture. The rat pancreatic exocrine cell line AR42J and the murine macrophage cell line RAW264.7 were obtained from Shanghai Institutes for Biological Sciences, The Cell Bank of Type Culture Collection (The Chinese Academy of Sciences), and were used in the experiments to evaluate the protective effects of BLN in the AP cell model. AR42J and RAW264.7 cells were plated in 25 cm^2 culture flasks at 37˚C in a humidified incubator supplied with 5% CO_2. AR42J cells were cultured in F12K supplemented with 20% FBS, while RAW264.7 cells were cultured in DMEM supplemented with 10% FBS. AR42J cells were passaged every 5-7 days, and RAW264.7 cells were passaged every 3-4 days. AR42J and RAW264.7 cells were subcultured at a ratio of 1:3 and 1:6, respectively, when they reached 80% confluency.

Establishment of the pancreatitis cell model. An AP cell model based on a patent (CN114250194A; http://epub.cnipa.gov.cn) was constructed. AR42J cells were exposed to F12K containing the toxins of HGO (25-50 mmol/l high glucose plus 100-400 μmol/l sodium oleate) at 37˚C for a duration of 24 h. MTT assays were used to evaluate the extent of cell damage. MTT solution (20 μl; 5 mg/ml) was added to each well. Following a 4-h incubation at 37˚C, the medium was replaced with 150 μl dimethyl sulfoxide to dissolve formazan crystals. Optical densities were measured at 490 nm with microplate reader (SpectraMax M2e; Molecular Devices).

Protective effect of BLN against HGO-induced cell damage. AR42J cells in the logarithmic phase were seeded in a 96-well plate (5x10^4 cells/well) and divided into seven groups after 24 h incubation at 37˚C. In the present study, five treatment groups were respectively pretreated with 1,000 U/ml ulinastatin (UTI), blank NPs (nanoparticles without BAPTA-AM), or 10, 50 or 250 nmol/l BLN for 0.5 h before HGO treatment. AR42J cells without any drug or HGO treatment were used as the normal control group, while cells exposed to HGO but not to BLN were considered the model group. A total of 24 h after HGO treatment, the protective effects of BLN against HGO-induced cell damage were evaluated using an MTT assay.

Inhibitory effect of BLN on HGO-induced cell apoptosis and necrosis. For collecting a sufficient quantity of cells, the AR42J cells were incubated in 6-well plates (1x10^6 cells/well) and divided into seven groups as aforementioned. After 24 h of exposure to HGO, the cells underwent gentle digestion (at 37˚C for 5 min) and centrifugation (300 x g for 4 min) at room temperature. Subsequently, the cells were rinsed twice with cold PBS before being resuspended in 500 μl binding buffer (2x10^5 cells). Following this, the cells were stained with 5 μl of Annexin V and 5 μl of PI from the kit at a temperature of 4˚C for 15 min in the dark. The Flow cytometer (FCM; FACSCanto II; BD Biosciences) and Flowjo V10 software (FlowJo LLC) were then used to determine the percentage of cells in the apoptotic stage.

Effect of BLN on intracellular Ca^{2+} overload. To investigate the Ca^{2+} scavenging effect of BLN on intracellular Ca^{2+} overload, intracellular Ca^{2+} levels were detected in AR42J cells following HGO-induced damage. Briefly, AR42J cells were seeded in 24-well plates (1x10^5 cells/well) and grouped as aforementioned. After 4 h HGO exposure, the culture medium was removed, cells were gently washed with D-Hanks buffer once and Fura-3/AM was added to a final concentration of 5 μmol/l. After incubated with Fura-3/AM for 2, 5, 10, 15 or 20 min, the cell images were respectively captured using an inverted fluorescence microscope (TE2000-U; Nikon Corporation). Image J (version 1.48; National Institutes of Health) was used to analyze the relative fluorescent intensity (RFI). The changes

in RFI in the cells represented the fluctuation of intracellular Ca^{2+} concentration.

Inhibitory effect of BLN on HGO-induced secretion of AMS from AR42J cells. AMS is primarily derived from pancreatic acinar cells and its excessive release is one of the characteristic indicators in the diagnosis of AP. The cells were divided and treated as described earlier, and the culture media was collected at 9 h after the HGO exposure. The detection of AMS in the culture media was performed in accordance with the protocol provided by the manufacturer.

Effect of BLN on HGO-induced ROS overproduction in AR42J cells. ROS are involved in numerous physiological processes. However, the overproduction of ROS also activates apoptotic pathways. After 9 h of HGO exposure, the ROS indicator 2',7'-Dichlorodihydrofluorescein diacetate (DCFH-DA) (1:1,000) was introduced to the AR42J cells following the guidelines provided by the manufacturer. When the cells were incubated with the fluorescent probe for another 30 min, the images of dichlorodihydrofluorescein (DCF) labeled cells were captured. Image J was used for quantitative analysis of the DCF fluorescence intensity. The areas with RFI values >15 and >35 were respectively regarded as the cell total and the region of ROS strongly positive cells.

Effect of BLN on the activation of inflammatory cells and overexpression of inflammatory cytokines. The RAW264.7 macrophage cell line is frequently used to explore inflammation. Upon being stimulated with LPS or cell debris, the macrophage cells were rapidly activated, and the release of various inflammatory cytokines, including IL-6 and TNF-α, amplifies the inflammatory response and further exacerbates existing cell damage. In the present study, the inhibitory effect of BLN on inflammatory responses was explored. The RAW264.7 cells were seeded in a 24-well plate and divided into seven groups. In addition to the normal group, the model, UTI, blank NP and BLN treatment groups were exposed to 100 ng/ml LPS or AR42J cell debris (~5,000 apoptotic or necrotic cells/ml) to induce inflammatory responses. The model group was exposed to the stimuli but without any pretreatment, while the normal group consisted of cells without the stimuli and BLN intervention. After a further 9 h of incubation, the culture media was collected. ELISA was performed to detect the expression of IL-6 and TNF-α according to the manufacturer's protocol. The remaining RAW264.7 cells were fixed with 4% paraformaldehyde at 4˚C for 15 min. After removing the fixative, a solution of Wright-Giemsa stain (0.5 ml) was added at room temperature incubated for 5 min. Subsequently, the staining solution was discarded, and the cells were washed three times with cold PBS before being observed under a light microscope (Nikon Eclipse Ti-S; Nikon Corporation) at a magnification of x200 to assess morphological changes.

Effect of BLN on inflammatory microenvironment induced AR42J cell apoptosis. The RAW264.7 cells were seeded in a 6-well plate at a density of $1x10^6$ cells/well. After incubating for 24 h, the cells were exposed to either LPS or AR42J cell debris. Then, the culture media were collected and centrifuged at room temperature (900 x g for 5 min). The supernatant, which was used to mimic an inflammatory microenvironment, was used for culturing the AR42J cells for a further 24 h. The AR42J cells cultured in supplemented DMEM were used as the normal control group, while the cells exposed to the aforementioned supernatant with or without BLN (250 nmol/l) were respectively defined as the model and BLN groups. FCM was used to determine the proportion of apoptotic cells.

Animal studies. Healthy Sprague-Dawley (SD) rats weighing 250±20 g and aged 8-10 weeks, with an equal distribution of males and females were purchased from the Zhejiang Center of Laboratory Animals (Hangzhou, China), and the experiments reported in the present study were performed in accordance with The Health Guide for Care and Use of Laboratory Animals, Zhejiang Center of Laboratory Animals. All animals were acclimated to the laboratory for ≥1 week before the experiments were performed and housed in a light-controlled room (12 h light/dark cycle) at an ambient temperature of 25˚C with *ad libitum* access to water and standard food.

Establishment of the sodium taurocholate (TC)-induced AP rat model. The *in vivo* retrograde injection of TC into the common biliopancreatic duct is a widely accepted experimental model for mimicking AP (33,34). This model involves a sequential process characterized by excessive activation and release of pancreatic enzymes, inflammatory cascades and eventually, pancreatic necrosis. The AP model in the present study was established as described by Aho *et al* (35) and Lange *et al* (36). A laparotomy in the midline was performed, using intraperitoneal injection of 2% sodium pentobarbital anesthesia at a dosage of 40 mg/kg (the anesthetic took effect within 15 min), and an injection needle was then inserted into the common biliopancreatic duct. The hepatic duct was closed using small hemostatic forceps and tightened with sutures around the needle and the wall of the duct. Steady manual pressure was applied to inject 0.2 ml saline or TC diluted in saline at a concentration of 4% into the pancreatic duct system for a period of >60 sec. Following a 5-min dwell time, the needle was removed after which the abdomen was sutured layer by layer.

Effect of BLN on the survival rate of the rats in the animal model of AP. A total of 64 rats were randomly allocated into the following eight groups, each consisting of eight animals: Normal, sham, model, UTI (20,000 U/kg), blank NP (NPs without BAPTA-AM) and three BLN treatment groups (75, 150 and 300 μg/kg). UTI is a trypsin inhibitor for treating AP and is included in the present study for comparison with BLN (37,38). All animals, except those in the normal group, underwent laparotomy and received either saline or TC solution injected into the common biliopancreatic duct, which connects the liver and pancreas. Mortality rates for each group were monitored at 0, 6, 12, 18, 24, 30, 36, 42 and 48 h after TC administration.

Effect of BLN on the biochemical indices. After being exposed to TC for 12 h or before sacrificing, 1.2-1.4 ml blood samples were collected and placed in an EP tube containing sodium citrate anticoagulant via tail-tip amputation. The expression levels of several indicators of pancreatic function, including

AMS, LDH, TGs, TNF-α and IL-6 in the serum were measured according to the manufacturer's protocol. At the experimental endpoint or prior to sacrifice, the rats were transferred to a CO_2 euthanasia chamber within their respective home cages and were euthanized using a CO_2 flow displacement rate of 30% per min. This process was continued until every rodent exhibited lack of respiration and faded eye color. Subsequently, the pancreas tissues were isolated and weighed. A portion of the tissues was used to prepare tissue homogenate to measure oxidative and anti-oxidative indicators, such as MDA, glutathione (GSH) and SOD.

Histopathological evaluation of the rescuing effect of BLN on AP. Histopathological changes in the pancreatic tissue can indicate the extent of necrosis. The pancreatic tissues were fixed in 10% buffering formalin at 4˚C for 24 h, embedded in paraffin, sliced into 5-μm-thick sections. The slices were subjected to a sequential washing procedure, commencing with xylene, followed by a series of ethanol solutions and distilled water. Subsequently, the sections were subjected to hematoxylin staining for a duration of 5 min at room temperature, followed by rinsing with tap water, and then stained with eosin staining solution for another 2 min. The slices were subsequently dehydrated and rendered transparent by sequential immersion in alcohol and xylene, and finally sealed with neutral gum. All pancreatic sections were observed using light microscopy (Nikon Eclipse Ti-S; Nikon Corporation), and images were captured in a blinded manner. Edema, inflammatory cell infiltration, hemorrhage, necrosis and other degenerative changes were used to assess pancreatic histology. The extent of pancreatic damage was graded on a scale from 0-III: 0, normal tissue; I, swelling can be observed in part of the pancreatic tissue but without obvious necrosis in the visual field; II, more swelling can be observed in the pancreatic tissue with visible spotty necrosis and inflammatory cell infiltration in the portal area, and necrosis in <1/2 of the area; and III, massive necrosis and swelling of the pancreatic tissue, and necrosis in >1/2 of the area (31,39,40).

Immunohistochemical analysis for TNF-α and cathepsin B protein expression. The premature activation of trypsinogen in pancreatic acinar cells, followed by the activation of other pancreatic zymogens, such as chymosinogen and prophospholipase, is considered to cause autodigestion of the gland, which is a crucial pathological change in AP (41,42). The mechanisms underlying trypsinogen activation in AP are not entirely clear. However, hypercalcemia, TNF-α and cathepsin B are hypothesized to play notable roles (43). TNF-α and cathepsin B can trigger both necrotic and apoptotic processes, which are mediated by receptor-interacting protein kinases. Meanwhile, TNF-α and cathepsin B are closely involved in inflammatory responses, which consist another type of pathological processes in AP. The pancreatic tissues were fixed with 10% buffered formalin, embedded in paraffin, and then sliced into 5 μm-thick sections. Immunohistochemical staining was performed using a standard peroxidase anti-peroxidase method, with diaminobenzidine (DAB) as the chromogen. After dewaxing and rehydration, sections were subjected to a citrate water bath at a temperature range of 96-98˚C for a duration of 15 min to recover antigens. To inhibit endogenous peroxidase activity, the sections were exposed to a 3% H_2O_2 solution at room temperature for 10 min. Additionally, nonspecific binding was prevented by treating the sections with 2% bovine serum albumin (BSA) at room temperature for 30 min. Subsequently, the sections were incubated with the primary antibody (dilution, 1:500) overnight at 4˚C, followed by incubation with the secondary antibody (dilution, 1:2,000) at room temperature for 10 min. Finally, the sections were stained with DAB. All slides were observed under a light microscope (Nikon Eclipse Ti-S; Nikon Corporation) and images were obtained for further analysis. The percentage of TNF-α and cathepsin B-stained areas (brown colored) was calculated using Image J. The proportion of positive area to total area was calculated and used as the relative expression level. The mean values from 10 fields of each section were taken as the individual rat score (31).

RNA isolation, cDNA synthesis and reverse transcription-quantitative (RT-q)PCR. The total RNA was extracted from pancreatic tissues using TRIzol® reagent (Thermo Fisher Scientific, Inc.), following the manufacturer's protocol. High-purity RNAs (2.0≥ A260/280 ≥1.8) were used for cDNA synthesis, with ≤0.8 μg RNA converted to cDNA based on the BioRT cDNA First Strand Synthesis kit (Hangzhou Bioer Technology Co., Ltd.) protocol, using RT temperature of 42˚C for 60 min. Gene transcription was quantified through qPCR using a Step One™ Real-Time PCR System (Applied Biosystems; Thermo Fisher Scientific, Inc.), along with template cDNA, forward/reverse primers and Maxima SYBR Green qPCR MasterMix reagent. The sequences of the primer are listed in Table SI. Thermocycling was carried out following the programmed procedure: Uracil DNA glycosylase pretreatment for 2 min at 50˚C, 5 min at 95˚C, followed by 40 cycles of 95˚C for 15 sec, 60˚C for 30 sec and 72˚C for 30 sec, with a final dissociation stage at 95˚C. After running SYBR Green PCR, data collection and analysis were performed with the fluorescence intensity (Rn) detected at the end of every cycle. The threshold cycle (C_q) values are inversely associated with the number of target cDNA copies. Quantification was calculated using the $2^{-\Delta\Delta Cq}$ value (44). C_q values of the target genes were compared with the C_q value of the endogenetic gene (EG) as follows: $\Delta C_q=C_q(TG)-C_q(EG)$ and $\Delta\Delta C_q=\Delta C_q(BLN)-C_q(Normal)$.

Statistical analysis. All data are presented as mean ± SD. One-way ANOVA followed by Dunnett's post hoc multiple comparison tests, two-way ANOVA followed by Tukey's post hoc multiple comparison tests and log-rank test were used to determine the significance of differences between experimental groups in GraphPad Prism (version 5.0; Dotmatics). $P<0.05$ was considered to indicate a statistically significant difference.

Results

Characterization of BLN. The morphology of BLN was visualized using SEM, as shown in Fig. 1A, revealing BLN to be spherical vesicles with a mean size of 113 nm. The size distribution was narrow, as confirmed by dynamic light scattering (Fig. 1B), with a mean diameter of 121.0±7.9 nm

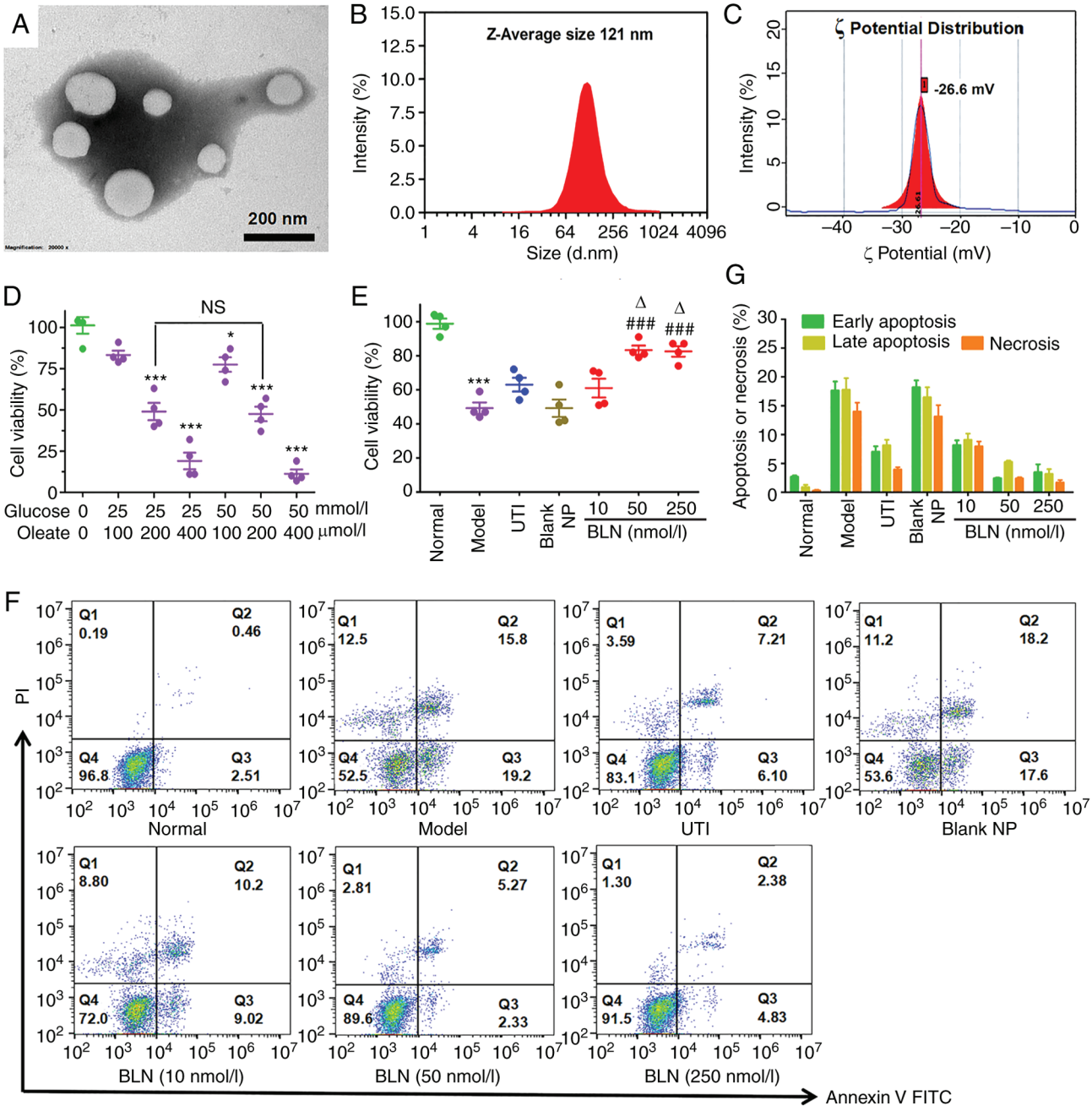

Figure 1. Characterization of BLN and its protective effect on HGO-induced AR42J cell damage. (A) Morphology of BLN using scanning electron microscopy. Scale bar, 200 nm. (B) Size distribution of BLN measured by DLS. (C) Surface charge of BLN. (D) Cytotoxicity screening of HGO in AR42J cells. (E) Cell viability of HGO-treated AR42J cells following BLN treatment measured using an MTT assay. (F) Cell apoptotic stages classified by flow cytometry. Early and late apoptotic cells are respectively presented in Q3 and Q2, necrotic cells in Q1 and normal cells in Q4. (G) Quantitative analysis for necrosis or apoptosis based on flow cytometry. *P<0.05, ***P<0.001 vs. normal group; $^{\#\#\#}$P<0.001 vs. model group, $^{\Delta}$P<0.05 vs. UTI group. Data are presented as the mean ± SEM of four repeats. BLN, BAPTA-AM loaded liposome nanoparticles; HGO, high glucose 25-50 mmol/l plus sodium oleate 100-400 μmol/l; DLS, dynamic light scattering; UTI, ulinastatin; NP, nanoparticle; BAPTA-AM, 1,2-bis(2-aminophenoxy)ethane-N,N,N',N'-tetraacetic acid tetrakis (acetoxymethyl ester).

and a PDI of 0.17±0.01, consistent with SEM measurements. The ζ potential of the BLN utilized in this experiment was -26.61±0.52 mV (Fig. 1C), a moderate potential for liposome stabilization. The encapsulation efficiency (EE) of BAPTA-AM was 95.3±2.1%. It was found that 7.5% trehalose (w/v) was an effective cryoprotectant for BLN. Notably, the lyophilization process did not significantly affect the size or the surface charge of BLN, and drug leakage was negligible upon reconstitution, facilitating long-term storage of this formulation (Table SII).

BLN prevents HGO-induced pancreatic acinar cell damage. As shown in Fig. 1D, HGO (25 mmol/l high glucose + 200 μmol/l sodium oleate) exposure resulted in a modest amount of cell damage, which was used to establish the AP cell model. Compared with the model group, the cell viability was significantly increased in the groups pretreated with BLN at a dose range of 10-250 nmol/l, particularly at a dose range of 50-250 nmol/l (Fig. 1E). FCM was also used to assess the viability of cells following BLN pretreatment. As shown in Fig. 1F and G, BLN pretreatment resulted in a significant

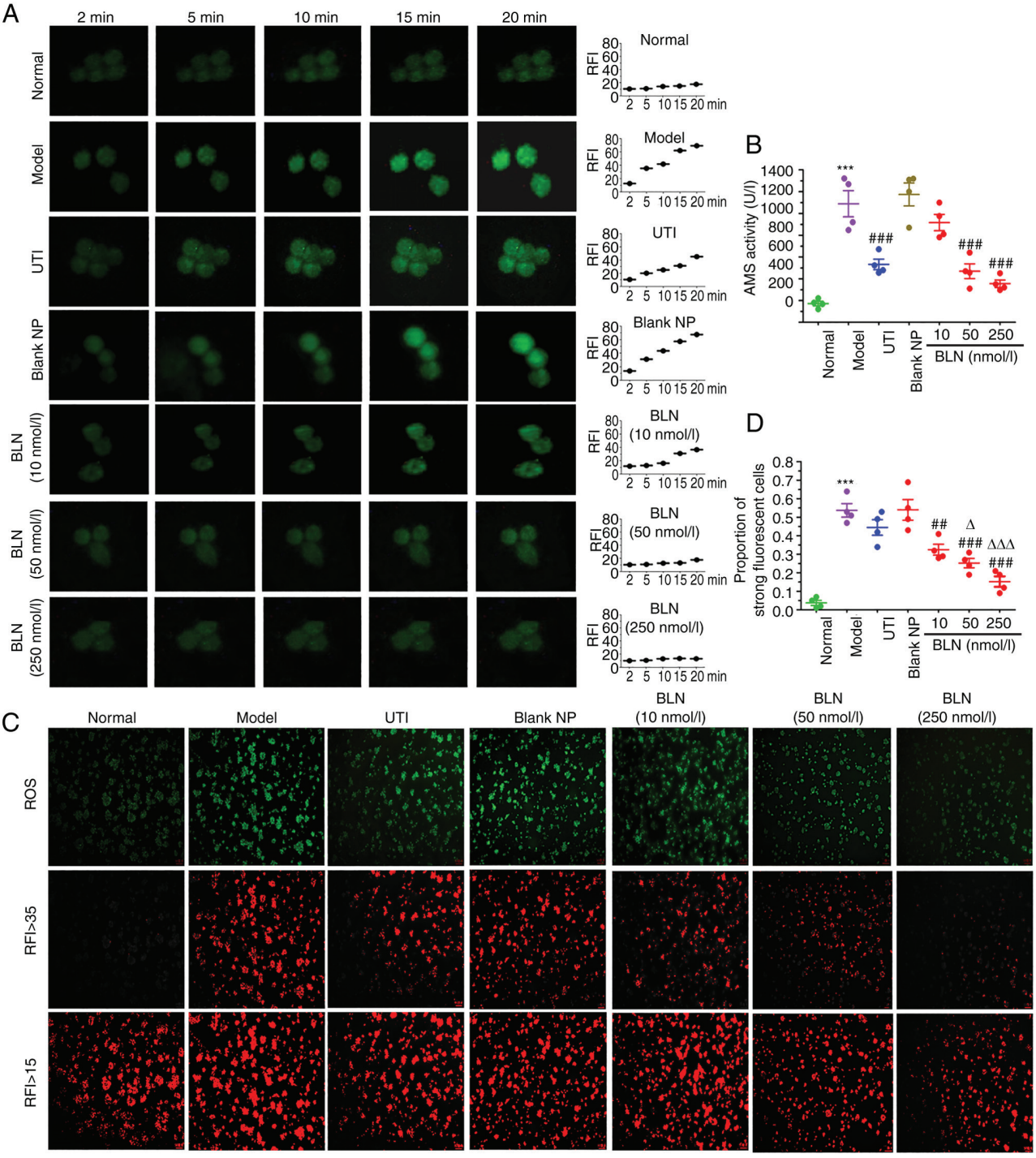

Figure 2. Inhibition of HGO-induced calcium overload, amylase over secretion, and ROS overproduction in AR42J cells. (A) Changes in intracellular [Ca^{2+}] in HGO-treated AR42J cells following BLN treatment. Scale bar, 5 μm. (B) BLN exhibited an inhibitory effect on HGO-induced amylase over secretion. (C) Representative images of ROS-induced fluorescence response; RFI values >15 and >35 were respectively regarded as the cell total and the region of ROS strongly positive cells. Scale bar, 100 μm. (D) Quantitative analysis of DCF relative fluorescence intensity. ***P<0.001 vs. normal group; $^{\#\#}$P<0.01, $^{\#\#\#}$P<0.001 vs. model group; $^{\Delta}$P<0.05, $^{\Delta\Delta\Delta}$P<0.001 vs. UTI group. Data are presented as the mean ± SEM of four repeats. BLN, BAPTA-AM loaded liposome nanoparticles; HGO, high glucose 25-50 mmol/l plus sodium oleate 100-400 μmol/l; UTI, ulinastatin; RFI, relative fluorescence intensity; ROS, reactive oxygen species; BAPTA-AM, 1,2-bis(2-aminophenoxy)ethane-N,N,N',N'-tetraacetic acid tetrakis (acetoxymethyl ester); NP nanoparticle; DCF, dichlorofluorescein; AMS, amylase.

reduction in the proportion of apoptotic or necrotic cells in a dose-dependent manner, which was consistent with the trend observed in the MTT assay.

BLN reduces Ca^{2+} overload in HGO-induced pancreatic acinar cell damage. The increase in Ca^{2+} levels in acinar cells is one of the initiating factors in the premature activation of zymogens and overproduction of ROS following HGO exposure (45,46). RFI was used to indicate the intracellular Ca^{2+} concentration. In the model group, a sudden increase in RFI was observed compared with the normal group, which suggested that the cells had become overloaded with Ca^{2+} in the model cells. Following BLN treatment, the RFI showed a dose-dependent decrease (Fig. 2A). Treatment with 50-100 nmol/l BLN reversed this

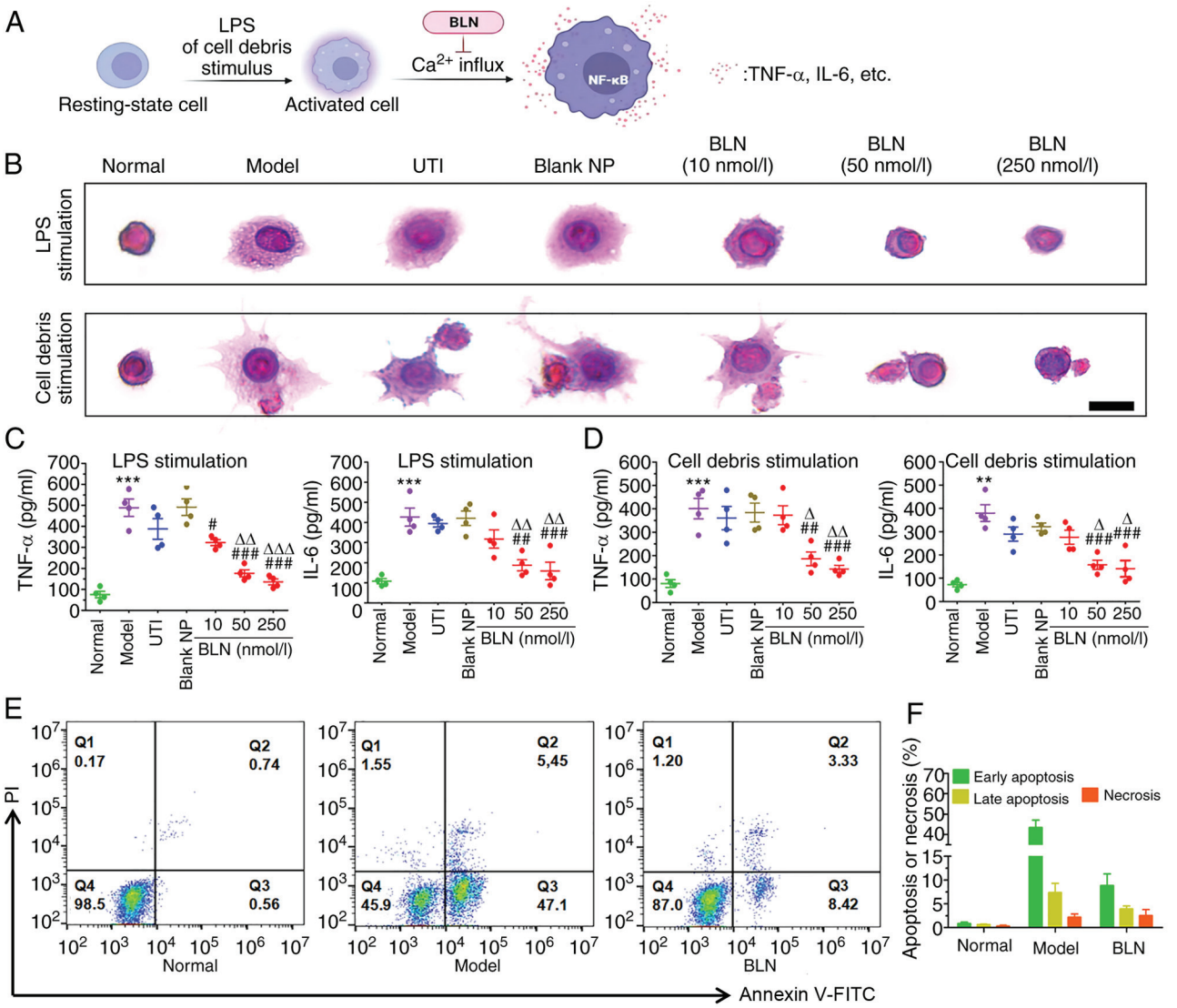

Figure 3. Inhibition of LPS and AR42J cell debris-stimulated inflammatory responses in RAW264.7 macrophages following BLN treatment. (A) Schematic diagram of the massive calcium influx promoting inflammatory cytokine release from activated monocytes. (B) LPS and cell debris-induced RAW264.7 cells morphological changes. Scale bar, 10 μm. (C) LPS and (D) cell debris exposure induced TNF-α and IL-6 expression in RAW264.7 cells. (E) Cell apoptotic stages classified by flow cytometry. (F) Quantitative analyses of necrosis or apoptosis based on flow cytometry. Data are presented as the mean ± SEM of four repeats. **P<0.01, ***P<0.001 vs. normal group, $^{\#}$P<0.05, $^{\#\#}$P<0.01, $^{\#\#\#}$P<0.001 vs. model group, $^{\Delta}$P<0.05, $^{\Delta\Delta}$P<0.01, $^{\Delta\Delta\Delta}$P<0.001 vs. UTI group. BLN, BAPTA-AM loaded liposome nanoparticles; UTI, ulinastatin; LPS, lipopolysaccharide; NP, nanoparticle; BAPTA-AM, 1,2-bis(2-aminophenoxy)ethane-N,N,N',N'-tetraacetic acid tetrakis (acetoxymethyl ester).

Ca^{2+} overload back to Ca^{2+} levels observed in the resting state. However, UTI did not result in the inhibition of Ca^{2+} influx. This result shows the potent Ca^{2+} scavenging ability of BLN, which is a prerequisite for the treatment of damaged cells.

BLN inhibits HGO-induced AMS oversecretion from AR42J cells. The abnormal elevation of plasma pancreatic AMS is an important indicator of pancreatitis (47,48). Excessive secretion and premature activation of pancreatin can lead to the autodigestion of pancreatic tissue, resulting in tissue bleeding and necrosis. The effects of BLN on AMS expression and release are shown in Fig. 2B. Compared with the normal group, AMS secretion in the culture media of the model group increased nearly 6-fold after 9 h of HGO co-incubation. However, pretreatment with BLN at dose range of 50-250 nmol/l significantly inhibited AMS expression by 57-70%.

BLN alleviates oxidative stress. Oxidative stress is regarded as a major causative factor in AP. To determine the effect of BLN on ROS production, intracellular ROS levels were assessed using DCF as a fluorescent indicator. Intracellular ROS levels were increased after 9 h of HGO exposure (Fig. 2C), with the majority of cells presenting strong yellow-green fluorescence. The proportion of area with RFI values ≥35 in the model group was 48-71%. BLN significantly suppressed ROS overproduction in a dose-dependent manner by 46-80% (Fig. 2D). These results indicated that BLN could reduce the cytotoxicity caused by ROS.

BLN inhibits LPS-induced inflammatory responses in RAW 264.7 macrophages. As shown in Fig. 3A and B, RAW264.7 cells exposed to LPS or AR42J cell debris for 9 h, exhibit a notable morphological change, characterized by mass

pseudopodia protrusions, indicating activation of the macrophages compared with the resting state observed in the cells in the normal group. This activation of inflammatory cells is a prerequisite for the release of inflammatory factors. Intervention with BLN (10-250 nmol/l) was found to have a notable anti-inflammatory effect and maintained the cells at rest in a dose-dependent manner. Inflammatory cytokines, such as TNF-α and IL-6, play a crucial role in AP initiation. As shown in Fig. 3C and D, TNF-α and IL-6 levels in RAW264.7 cells exposed to 100 ng/ml LPS or AR42J cell debris were significantly increased up to 3-8-fold the normal level. However, BLN treatment significantly inhibited the inflammatory responses, especially when the cells were treated with BLN at concentrations ≥50 nmol/l. UTI did not alleviate the inflammatory responses. Furthermore, the inflammatory microenvironment aggravated apoptosis. The supernatant rich in TNF-α and IL-6 from activated RAW264.7 cell culture medium significantly promoted the occurrence of apoptosis. BLN (250 nmol/l) blocked this apoptotic process (Fig. 3E and F). These results suggest that BLN treatment can effectively prevent macrophage activation and block LPS or cell debris-stimulated inflammatory responses. These findings highlight the protective effect of BLN against cell apoptosis or necrosis.

Table I. Effects of BLN on the pathological grade of TC-assaulted rats (n=8).

	Grade				
Group	0	I	II	III	P-value
Normal	8	0	0	0	
Sham	8	0	0	0	NS
Model	0	0	2	6	[a]
UTI	2	5	1	0	[b]
Blank NP	0	1	3	4	NS[a]
BLN (75 μg/kg)	1	5	2	0	[b]
BLN (150 μg/kg)	3	5	0	0	[b]
BLN (300 μg/kg)	5	3	0	0	[b]

[a]P<0.001 vs. normal group; [b]P<0.001 vs. model group; NS, not significant vs. normal group; NS[a], not significant vs. model group. BLN, BAPTA-AM loaded liposome nanoparticles; UTI, ulinastatin; NP, nanoparticles; BAPTA-AM, 1,2-bis(2-aminophenoxy) ethane-N,N,N',N'-tetraacetic acid tetrakis (acetoxymethyl ester).

Effect of BLN on the survival rate in the animal model of AP. AP is characterized by a rapid deterioration in health and a high mortality rate. As shown in Fig. 4A, the survival rate of the model group decreased sharply after the first death occurred 12 h post-TC assault via retrograde injection of TC into the pancreatic duct. The survival rate plummeted to 50% after 24 h and to 37.5% after 48 h. However, BLN (75-300 μg/kg) treatment significantly extended the survival time, and no TC-treated rats died in the first 24 h, which is a critical period for rescuing patients with AP. Treatment with BLN at a dose of 150 μg/kg resulted in a terminal survival rate of 75% at the experimental endpoint, a significant improvement compared with the model group's rate of only 37.5%. Furthermore, BLN (150 μg/kg) had a superior rescuing effect compared with that of UTI, a commonly used pancreatic protective agent in clinical settings.

Measurement of serum and homogenate biochemical indices. Increases in serum AMS, LDH, and TG serve as important diagnostic indicators of AP, while MDA, GSH and SOD in homogenates are the most commonly used indices to inspect oxidative injury (48,49). All biomarker levels in the sham and normal groups did not differ notably, indicating normal pancreatic function in these groups. By contrast, the AP model group showed notably increased levels of serum AMS, LDH, TG and homogenate MDA by 3-6-fold after 24 h, displaying a significant reduction in antioxidant levels of homogenate GSH and SOD, when compared with the normal group, suggesting a notable decrease in pancreatic function. Treatment with BLN resulted in a dose-dependent recovery in pancreatic function compared with the model group (Fig. 4B-G). Taken together, these results suggest that BLN exhibits excellent therapeutic effects in the rat model of AP.

Improvement of serum inflammatory cytokines. ELISA was used to quantitatively analyze the levels of TNF-α and IL-6 in serum (Fig. 4H and I). As early contributors to AP events, TNF-α and IL-6 play a crucial role in the process of the inflammatory cascade, apoptosis and necrosis. After 12 h of modeling, a significant increase in TNF-α and IL-6 expression was observed, which was 4-6-fold higher than that in the normal group. By contrast, the TNF-α and IL-6 levels in the BLN treatment groups were significantly lower; <30% of those in the model group. These findings suggest that BLN has the potential to protect the pancreas by exhibiting anti-inflammatory and anti-apoptotic properties.

Alleviation of the pancreatic destruction. Based on the aforementioned experimental results, pancreatic tissues were chosen for H&E staining to explore the pathological changes (Fig. 4J and Table I). Both the normal group and the sham group exhibited no histological abnormalities, as evidenced by the presence of an intact pancreatic structure and well-preserved cytoplasm (grade 0). However, the histopathological results for the AP model group revealed a notable amount of destruction, including a considerable amount of necrosis, inflammatory infiltrates, cellular swelling and vacuolization (grade II and III). Despite exhibiting mild swelling, the histological structure of the pancreatic tissue in the BLN treatment group did not show visibly abnormal regions. After BLN treatment, the injury degree was significantly decreased in a dose-dependent manner to mainly grade 0 and I.

Modulation of the expression of pro-apoptotic and pro-necrotic cytokines. The inflammatory response associated with AP promotes an increase in the expression of two important cytokines, namely TNF-α and cathepsin B, leading to the initiation of apoptotic or necrotic signaling pathways (50-53). The binding of TNF-α to its receptor TNFR-1 stimulates the release of cathepsin B from lysosomes, which then promotes the activation of the apoptotic or necrotic pathways. Thus, lower levels of these cytokines

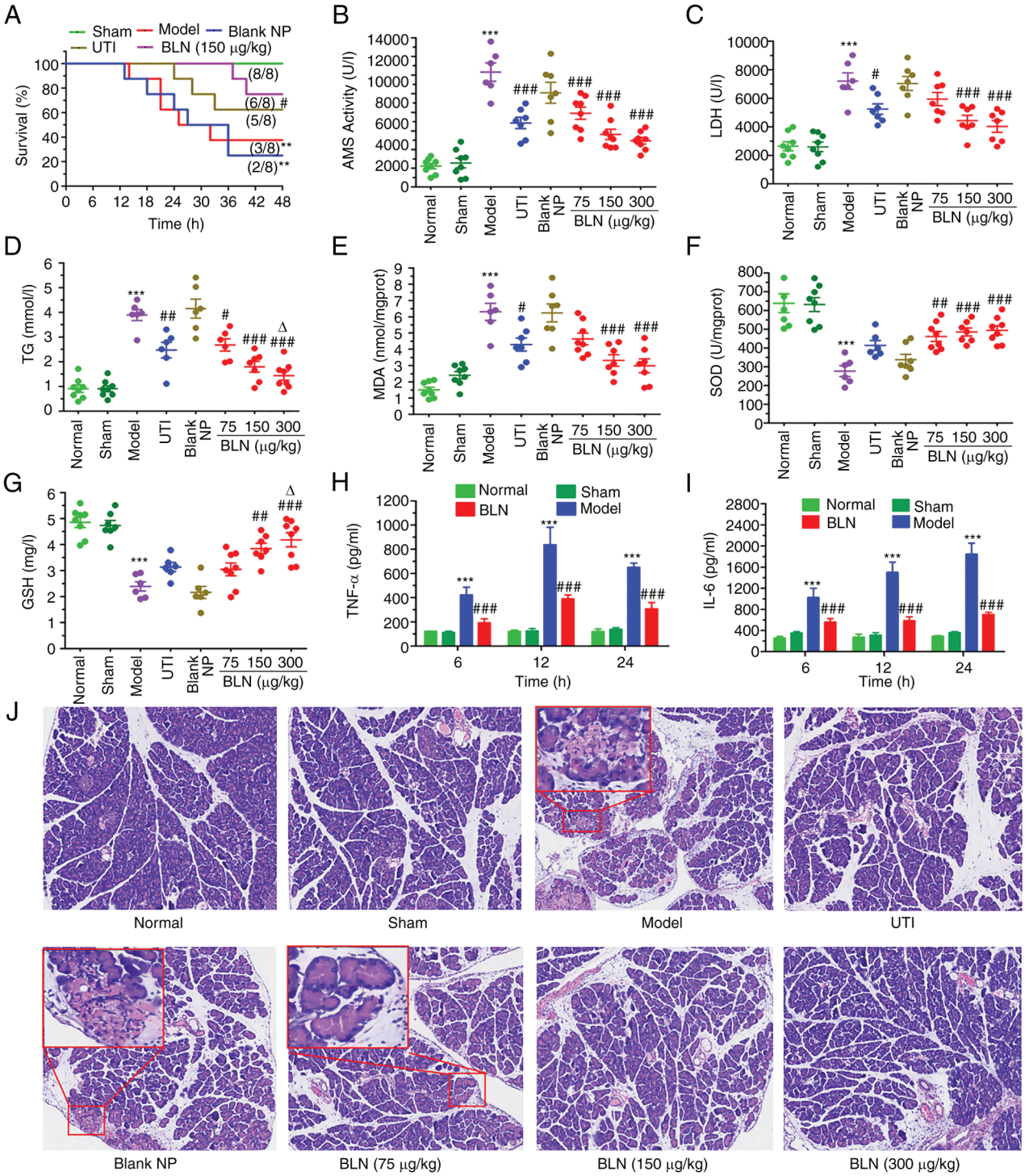

Figure 4. Effects of BLN on the survival rate, biomarker levels, and inflammatory cytokine levels. (A) The change in survival rates in different groups was monitored for 48 h following BLN treatment. Levels of (B) AMS, (C) LDH, and (D) TG in serum and (E) MDA, (F) SOD and (G) GSH levels in the pancreas homogenates from different groups after 12 h of BLN treatment. Levels of (H) TNF-α and (I) IL-6 levels in serum. (J) Pancreatic histological observation of the different experimental groups. Original magnification, x100. Data are presented as the mean ± SEM of eight repeats. **P<0.01, ***P<0.001 vs. normal group, $^{\#}$P<0.05, $^{\#\#}$P<0.01, $^{\#\#\#}$P 0.001 vs. model group, $^{\Delta}$P<0.05 vs. UTI group. BLN, BAPTA-AM loaded liposome nanoparticles; UTI, ulinastatin; LPS, lipopolysaccharide; NP, nanoparticle; BAPTA-AM, 1,2-bis(2-aminophenoxy)ethane-N,N,N',N'-tetraacetic acid tetrakis (acetoxymethyl ester); AMS, amylase; LDH, lactate dehydrogenase; TG, triglyceride; MDA, malondialdehyde; SOD, superoxide dismutase; GSH, glutathione.

indicate a reduction in pancreatic acinar cell damage by inhibiting these signaling pathways. The levels of TNF-α and cathepsin B were assessed using immunohistochemistry and western blotting. As shown in Fig. 5A, there was a sharp increase in TNF-α and cathepsin B expression in the pancreatic tissues of the model group, suggesting the onset of apoptosis or necrosis. However, treatment with BLN effectively and rapidly reduced the expression of these cytokines, leading to a 50-70% decrease in TNF-α and cathepsin B levels (Fig. 5B and C). Western blotting was also used to verify the anti-apoptotic or anti-necrotic effects of BLN, and the results of western blotting were consistent with those of

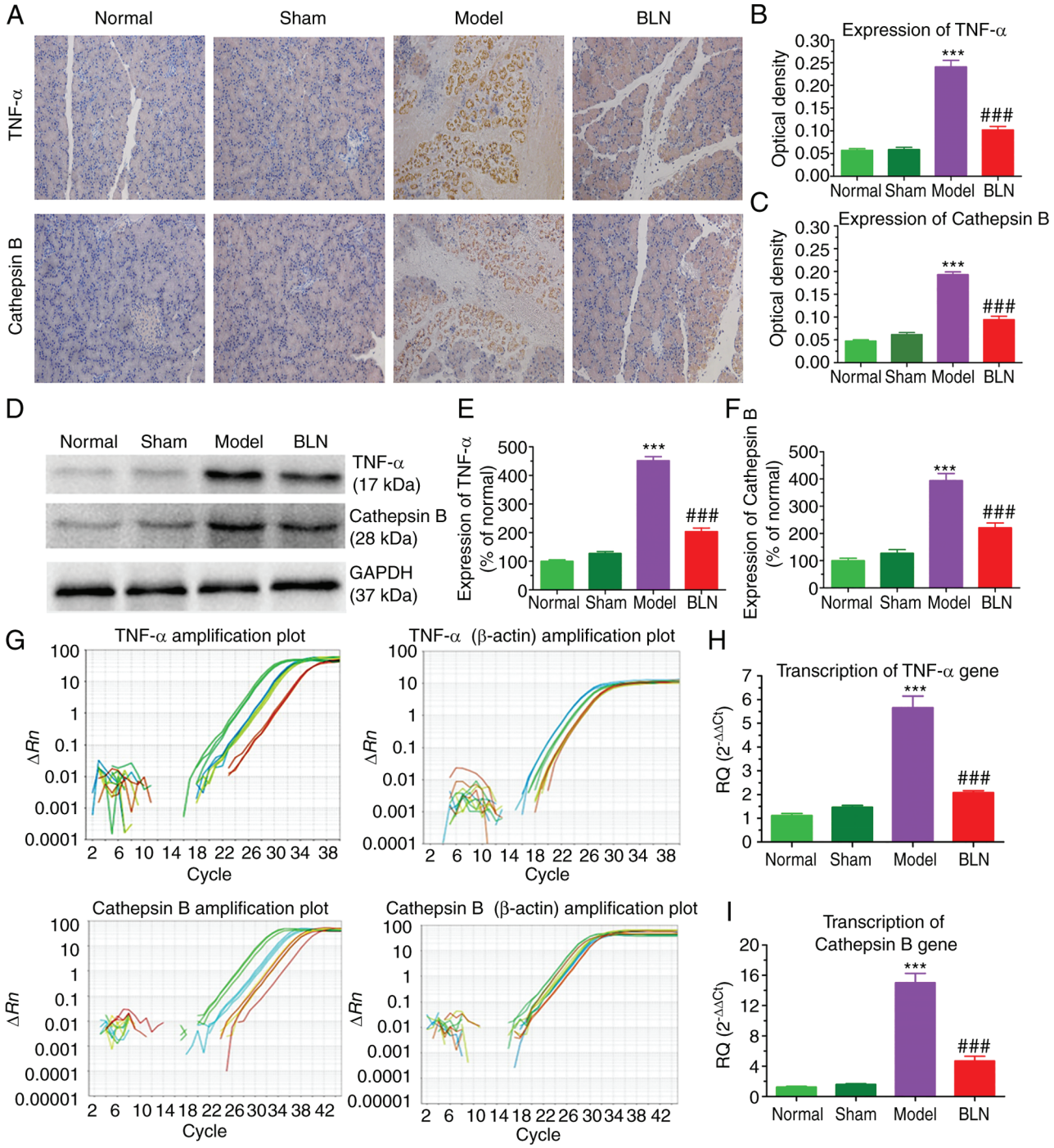

Figure 5. Effects of BLN on TNF-α and cathepsin B expression. (A) Immunohistochemical staining for TNF-α and cathepsin B protein. Original magnification, x200. TNF-α or cathepsin B positive areas are colored brown. Expression levels of (B) TNF-α and (C) cathepsin B calculated based on immunohistochemical staining. (D) TNF-α and cathepsin B levels in pancreas homogenate determined by western blotting. (E and F) Quantitative analysis of TNF-α and cathepsin B expression based on western blotting. (G) mRNA transcription levels of TNF-α and cathepsin B. (H and I) Quantitative analysis of TNF-α and cathepsin B mRNA expression levels. Data are presented as the mean ± SEM of three repeats. ***P<0.001 vs. normal group; $^{###}$P<0.001 vs. model group. BLN, BAPTA-AM loaded liposome nanoparticles; BAPTA-AM, 1,2-bis(2-aminophenoxy)ethane-N,N,N',N'-tetraacetic acid tetrakis (acetoxymethyl ester).

immunohistochemistry (Fig. 5D-F). Therefore, BLN may exert its therapeutic effect by inhibiting a TNF-α/cathepsin B signaling pathway to reduce pancreatic acinar cell damage in AP.

Inhibition of pro-apoptotic and pro-necrotic gene transcription. As shown in Fig. 5G, the association between the cycles of PCR and fluorescence intensity followed an ideal amplification curve, with an S-shaped pattern. The genes of TNF-α, cathepsin B and β-actin, displayed clear phases of exponential amplification and plateauing. The qPCR data of this experiment were sufficient for the quantitative analysis of TNF-α, cathepsin B and β-actin genes, and a wide linear range of association was detectable in the 14th-32nd cycles. Amplification of a specific vs. non-specific product could be differentiated through dissociation curve analysis. The dissociation curves

of TNF-α and cathepsin B gene amplification products with a single peak indicated specific amplification for TNF-α and cathepsin B genes, free from primer-dimers or other impurities. TNF-α and cathepsin B gene melting temperatures were 81.86˚C and 80.21˚C, respectively (Fig. S3). Compared with the normal group, the transcription of TNF-α and cathepsin B mRNA in the pancreas tissue of the model group increased by a factor of 5-10. However, TNF-α and cathepsin B mRNA were significantly reduced by 57-73% in the BLN treatment group (150 μg/kg; Fig. 5H and I). In conjunction with the aforementioned data, it was postulated that the rapid suppression of the TNF-α/cathepsin B signaling pathway subsequent to BLN treatment significantly contributed to the therapeutic efficacy for AP.

Discussion

AP is an acute inflammatory process localized to the pancreas in clinical practice with a high mortality rate characterized by the premature activation of zymogens, causing pancreatic tissue edema, hemorrhage and necrosis (54,55). Intracellular Ca^{2+} overload is generally accepted as a key trigger initiating pancreatic acinar cell damage (27,56,57). The aberrant Ca^{2+} elevation in acinar cells can not only provoke the fusion of zymogen granules with lysosomes to activate the cleavage of trypsinogen to trypsin causing pancreatic autodigestion (58), but also induces the overproduction of oxygen radicals that further target and damage the cytoplasmic and mitochondrial membrane (27,59). The results of the present study also showed that inhibiting intracellular Ca^{2+} overload could simultaneously reduce pancreatic enzyme premature activation and mitigate oxidative stress injury. However, it is not clear whether Ca^{2+} overload directly promotes the activation and release of pancreatic enzymes, the exact mode of the BAPTA action must be interpreted with caution. The conclusions of Wang *et al* (60) and those of the current study suggest that Ca^{2+} chelators can reduce acute pancreatic cell injury by inhibiting the expression of inflammatory factors which could induce the activation of protrypsin. In addition, the activation of Ca^{2+}-dependent proteases, such as calpain, due to the Ca^{2+} elevation, is known to have a substantial impact on the development of cell damage induced by oxidative stress. Chelation of intracellular Ca^{2+} leads to complete inhibition of H_2O_2-induced proteolytic activity (16). ROS and Ca^{2+} overload mutually reinforce each other, forming a feedback loop (61). The pair can further activate macrophages to release inflammatory cytokines, such as TNF-α and IL-6, which amplifies the inflammatory cascade, and eventually leads to further deterioration of the local tissue and aggravate AP (62,63). These cytokines increase the capillary permeability and promote inflammatory infiltration. The binding of TNF-α to its receptor TNF-R1 contributes to the maturation and release of cathepsin B from lysosomes, which subsequently triggers the cathepsin B-mediated apoptotic or necroptotic pathway (50,64). Thus, intracellular Ca^{2+} overload plays a pivotal role in the occurrence and development of AP. Rapidly restoring Ca^{2+} to the resting state is useful for lessening the excessive activation of zymogens, halting the inflammatory progression and ameliorating pathological acinar cell apoptosis and necrosis (65).

To mimic hyperlipidemia or gallstone-related pancreatitis, two well-characterized models were used in the present study: An *in vitro* model of HGO-induced AR42J cell damage and an *in vivo* model of intra-ductal taurocholate infusion-induced AP (66). These models involve stepwise processes characterized by an excessive release of pancreatic enzymes, severe inflammatory responses and fulminant pancreatic necrosis, which are consistent with the clinical manifestations of severe pancreatitis. Of note, inflammatory cells, such as macrophages and neutrophils, are intricately involved in the process of AP development. The simple restriction of zymogen activation is insufficient to rescue the endangered acinar cells due to the release/induction of pancreatic toxins (ROS, LPS and Ca^{2+} overload) provoking inflammatory cytokine overproduction, which thus exacerbates cell damage. Since the absence of anti-inflammatory and anti-apoptotic functions, the rescuing functions for severe AP of the available anti-pancreatitis drugs (such as somatostatin and gabexate) are less than satisfactory. Following intervention with somatostatin or gabexate, ~20% of patients with AP still progress to SAP, which is characterized by a systemic inflammatory response. In clinical practice, there is a high mortality of 20-40% for patients with SAP with currently available anti-pancreatitis regimens.

Clinically, the therapeutic regimen for AP typically involves symptomatic therapy, such as fluid resuscitation, low-fat diet, antibiotic therapy and biliary drainage, rather than etiological treatment (67,68). Reversing the Ca^{2+} overload in the endangered acinar cells while simultaneously inhibiting monocyte activation may be a more feasible scheme for curing AP. Compared to the Ca^{2+} channel blockers, BAPTA-AM can more effectively and rapidly reverse the overload in intracellular Ca^{2+} concentration to a resting state (69,70). BAPTA-AM is hydrolyzed by lipases into BAPTA within acinar cells, and in this hydrolyzed form, it decreases the degree of Ca^{2+} overload. In an ischemia/reperfusion-induced acute kidney injury model, the use of BAPTA-AM loaded NPs effectively impedes Ca^{2+} overload and hinders the activation of the endoplasmic reticulum stress cascade response while interrupting the feedback loop between Ca^{2+} overload and ROS, thereby mitigating oxidative stress-induced damage (32,28,61). In our previous study, it was also validated that BLN exhibited a beneficial protective impact on fulminant hepatic failure induced by D-GalN/LPS via a comparable mechanism of action (31). BAPTA-AM prevented various types of fulminant necrosis by protecting against oxidative damage, maintaining the mitochondrial membrane potential and suppressing both endogenous and exogenous apoptotic pathways (71-74). AP is also considered a fulminant and necrotizing disease (75,76). The results of the current study suggest that BLN could not only disrupt the reciprocal relationship between Ca^{2+} overload and ROS, but also delay the macrophage activation to block the inflammatory cascades. These potential mechanisms can correspondingly fight against the pathological process of AP.

In the present study, the rescuing functions of BLN were further demonstrated *in vitro* and *in vivo* AP models. HGO exposure results in a pathological rise in cytosolic Ca^{2+} in AR42J cells, which triggers the excessive release of AMS, which is a specific indicator for the diagnosis of AP (77,78).

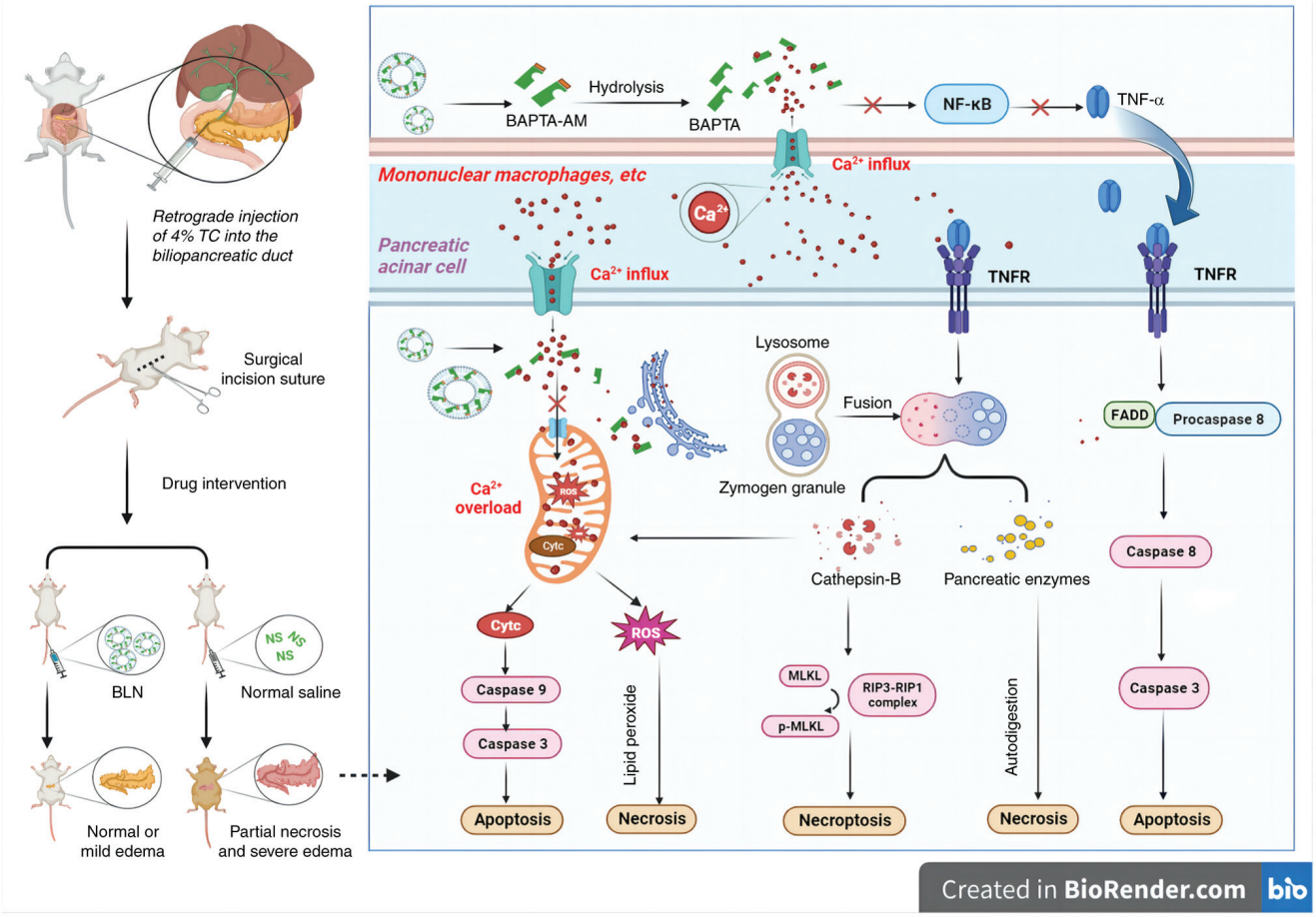

Figure 6. Schematic illustration of proposed mechanism by which BLN protects pancreatic cells in the rat model of AP through preventing the intracellular calcium overload. AP, acute pancreatitis; BLN, BAPTA-AM loaded liposome nanoparticles; BAPTA-AM, 1,2-bis(2-aminophenoxy)ethane-N,N,N',N'-tetraacetic acid tetrakis (acetoxymethyl ester); p, phosphorylated; TC, sodium taurocholate; ROS, reactive oxygen species; MLKL, mixed lineage kinase domain like protein; RIP, receptor interaction protein; FADD, fas-associating protein with death domain.

Furthermore, intracellular Ca^{2+} overload can promote excessive ROS production in pancreatic acinar cells, leading to oxidative stress. Ca^{2+} influx and oxidative stress self-amplify and potentiate each other until mass cell death is observed (31). In addition to the aforementioned pathological changes, the inflammatory cascade is another characteristic of SAP. There is sufficient evidence that inflammatory mediators, such as IL-6 and TNF-α, are closely involved in the progression of AP (79,80). The endotoxin and acinar cellular contents from collapsed cells recruit inflammatory cells to infiltrate the pancreas and augment the inflammatory responses. The RAW264.7 macrophage cell line, which is frequently employed to explore inflammation, releases mass quantities of inflammatory cytokines following endotoxin stimulation. In the present study, it was found that BLN not only inhibited the premature activation of zymogens and oxidative stress caused by Ca^{2+} overload, but also relieved inflammatory damage. These results illustrated that Ca^{2+} overload was a key trigger in the progression of AP. Rapid elimination of Ca^{2+} overload is beneficial to the rescue of the pancreas. The results of the present study suggested that BLN exerted a promising protective effect on a rat model of AP, increasing the survival rate from 37.5 to 75%. BLN exhibited considerably better therapeutic outcomes compared with those of UTI, a currently available pancreatic protective agent (81). BLN recovered pancreatic microcirculation and the function of the pancreas by improving blood biochemistry indices, alleviating oxidative damage, restricting the activation of trypsinogen and downregulating the expression of TNF-α and IL-6. Pancreatic histopathology scores showed that BLN significantly relieved pancreatic damage. According to the immunohistochemistry and RT-qPCR results, it was found that the substantial increase in the levels of cathepsin B was also involved in the rapid development of AP, boosting the progression of pancreatic acinar cell necroptosis. In addition to the ability of BLN to block TNF-α-mediated endogenous apoptotic pathways, BLN also notably reduced the cathepsin B burden. The multifaceted interventional mechanisms of BLN for the prevention of cellular death may underlie its rescuing effects.

In conclusion, BLN exhibits significant promise as an innovative therapeutic approach for managing AP. Its ability to promptly mitigate intracellular Ca^{2+} overload can greatly enhance survival rates and restore pancreatic function. The underlying pancreas protective mechanism of BLN is primarily attributed to its potent anti-necrotic and anti-apoptotic properties for pancreatic acinar cells, which are achieved through the prevention of premature trypsinogen activation, mitigation of oxidative damage and inhibition of apoptotic or necrotic pathways mediated by TNF-α and cathepsin B (Fig. 6). It was hypothesized that regulating intracellular Ca^{2+} concentration

and preventing Ca^{2+} overload would be a promising strategy for alleviating acute pancreatic damage. Furthermore, the cell rescue capability of BLN suggests its potential application in treating other severe diseases characterized by extensive cellular damage such as stroke and hepatic encephalopathy. Notably, compared with UTI, a marketed trypsin and serine protease inhibitor, BLN exhibited superior therapeutic outcomes that strongly support its future clinical translational potential. In theory, the synergistic effects of BLN with protease inhibitors and antioxidants can cute AP. To further enhance the potential efficacy of this drug, future research will focus on optimizing carrier design to achieve optimal therapeutic effects.

Acknowledgements

Not applicable.

Funding

The present study was supported by Zhejiang Province Medical and Health Science and Technology Project (grant no. 2020370024) and the Joint Funds of the Zhejiang Provincial Natural Science Foundation of China under Grant (grant no. LYY21H310007).

Availability of data and materials

The data generated in the present study may be requested from the corresponding author.

Authors' contributions

ZF, YS and WH conceived and planned the study. ZF, DW, CZ, MX, YC, YZ and YH conducted all experiments and performed data analysis and interpretation. ZF, WH and CZ confirm the authenticity of all the raw data. ZF, YS and WH wrote the manuscript, which was reviewed and edited by all co-authors. All authors have read and approved the final version of the manuscript.

Ethics approval and consent to participate

The animals used in the present study were provided by the Zhejiang Center of Laboratory Animals [number of quality certification, SCXK(zhe)-2021-0002; number of experimental facilities certification, SYXK(zhe)-2022-0005]. Animal experiments were approved by the Animal Experiments Ethical Inspection of Zhejiang Center of Laboratory Animals (approval no. 2022R0006). All animal studies complied with the Health Guide for Care and Use of Laboratory Animals, Zhejiang Center of Laboratory Animals.

Patient consent for publication

Not applicable.

Competing interests

The authors declare that they have no competing interests.

References

1. Chan YC and Leung PS: Acute pancreatitis: Animal models and recent advances in basic research. Pancreas 34: 1-14, 2007.
2. Jia A, Yang Z, Shi J, Liu J, Zhang K and Cui Y: MiR-325-3p alleviates acute pancreatitis via targeting RIPK3. Digest Dis Sci 67: 4471-4483, 2022.
3. Zhao Q, Zhang H, Huang J, Yu H, Li J, Che Q, Sun Y, Jin Y and Wu J: Melatonin attenuates the inflammatory response via inhibiting the C/EBP homologous protein-mediated pathway in taurocholate-induced acute pancreatitis. Int J Mol Med 42: 3513-3521, 2018.
4. Baron TH, DiMaio CJ, Wang AY and Morgan KA: American gastroenterological association clinical practice update: Management of pancreatic necrosis. Gastroenterology 158: 67-75, 2020.
5. Boxhoorn L, Voermans RP, Bouwense SA, Bruno MJ, Verdonk RC, Boermeester MA, van Santvoort HC and Besselink MG: Acute pancreatitis. Lancet 396: 726, 2020.
6. Heckler M, Hackert T, Hu K, Halloran CM, Büchler MW and Neoptolemos JP: Severe acute pancreatitis: Surgical indications and treatment. Langenbecks Arch Surg 406: 521-535, 2021.
7. Leppaniemi A, Tolonen M, Tarasconi A, Segovia-Lohse H, Gamberini E, Kirkpatrick AW, Ball CG, Parry N, Sartelli M, Wolbrink DRJ, *et al*: 2019 WSES guidelines for the management of severe acute pancreatitis. World J Emerg Surg 14: 27, 2019.
8. Crockett SD, Wani S, Gardner TB, Falck-Ytter Y, Barkun AN, Crockett S, Falck-Ytter Y, Feuerstein J, Flamm S, Gellad Z, *et al*: American gastroenterological association institute guideline on initial management of acute pancreatitis. Gastroenterology 154: 1096-1101, 2018.
9. Portelli M and Jones CD: Severe acute pancreatitis: Pathogenesis, diagnosis and surgical management. Hepatob Pancreat Dis 16: 155-159, 2017.
10. Bang U, Semb S, Nojgaard C and Bendtsen F: Pharmacological approach to acute pancreatitis. World J Gastroenterol 14: 2968-2976, 2008.
11. Moggia E, Koti R, Belgaumkar AP, Fazio F, Pereira SP, Davidson BR and Gurusamy KS: Pharmacological interventions for acute pancreatitis. Cochrane Database Syst Rev 4: D11384, 2017.
12. Ward JB, Jenkins SA, Sutton R and Petersen OH: Is an elevated concentration of acinar cytosolic free ionised calcium the trigger for acute pancreatitis? Lancet 346: 1016-1019, 1995.
13. Mithöfer K, Fernández-Del Castillo C, Frick TW, Lewandrowski KB, Rattner DW and Warshaw AL: Acute hypercalcemia causes acute pancreatitis and ectopic trypsinogen activation in the rat. Gastroenterology 109: 239-246, 1995.
14. Sakorafas GH and Tsiotou AG: Etiology and pathogenesis of acute pancreatitis: Current concepts. J Clin Gastroenterol 30: 343-356, 2000.
15. Yang AL and McNabb-Baltar J: Hypertriglyceridemia and acute pancreatitis. Pancreatology 20: 795-800, 2020.
16. Weber H, Huhns S, Luthen F, Jonas L and Schuff-Werner P: Calpain activation contributes to oxidative stress-induced pancreatic acinar cell injury. Biochem Pharmacol 70: 1241-1252, 2005.
17. Orrenius S, Ankarcrona M and Nicotera P: Mechanisms of calcium-related cell death. Adv Neurol 71: 137, 1996.
18. Orrenius S, Gogvadze V and Zhivotovsky B: Calcium and mitochondria in the regulation of cell death. Biochem Bioph Res Commun 460: 72-81, 2015.
19. Gerasimenko J, Peng S and Gerasimenko O: Role of acidic stores in secretory epithelia. Cell Calcium 55: 346-354, 2014.
20. Xiao J, Lin H, Liu B and Jin J: CaMKII/proteasome/cytosolic calcium/cathepsin B axis was present in tryspin activation induced by nicardipine. Biosci Rep 39: BSR20190516, 2019.
21. Xie Z, Zhao M, Yan C, Kong W, Lan F, Narengaowa, Zhao S, Yang Q, Bai Z, Qing H and Ni J: Cathepsin B in programmed cell death machinery: Mechanisms of execution and regulatory pathways. Cell Death Dis 14: 255, 2023.
22. Reinheckel T, Deussing J, Roth W and Peters C: Towards specific functions of lysosomal cysteine peptidases: Phenotypes of mice deficient for cathepsin B or cathepsin L. Biol Chem 382: 735, 2001.
23. Sendler M, Dummer A, Weiss FU, Krüger B, Wartmann T, Scharffetter-Kochanek K, van Rooijen N, Malla SR, Aghdassi A, Halangk W, *et al*: Tumour necrosis factor α secretion induces protease activation and acinar cell necrosis in acute experimental pancreatitis in mice. Gut 62: 430-439, 2013.

24. Dawra R, Sah RP, Dudeja V, Rishi L, Talukdar R, Garg P and Saluja AK: Intra-acinar Trypsinogen activation mediates early stages of pancreatic injury but not inflammation in mice with acute pancreatitis. Gastroenterology 141: 2210-2217, 2011.
25. Shen Y, Malik SA, Amir M, Kumar P, Cingolani F, Wen J, Liu Y, Zhao E, Farris AB, Raeman R, *et al*: Decreased hepatocyte autophagy leads to synergistic IL-1β and TNF mouse liver injury and inflammation. Hepatology 72: 595-608, 2020.
26. Wu H, Zhang M, Li W, Zhu S and Zhang D: Stachydrine attenuates IL-1β-induced inflammatory response in osteoarthritis chondrocytes through the NF-κB signaling pathway. Chem Biol Interact 326: 109136, 2020.
27. Criddle DN: Reactive oxygen species, Ca(2+) stores and acute pancreatitis; a step closer to therapy? Cell Calcium 60: 180-189, 2016.
28. Wang Y, Pu M, Yan J, Zhang J, Wei H, Yu L, Yan X and He Z: 1,2-Bis(2-aminophenoxy)ethane-N,N,N',N'-tetraacetic Acid Acetoxymethyl ester loaded reactive oxygen species responsive hyaluronic acid-bilirubin nanoparticles for acute kidney injury therapy via alleviating calcium overload mediated endoplasmic reticulum stress. ACS Nano 17: 472-491, 2023.
29. Quarato G, Llambi F, Guy CS, Min J, Actis M, Sun H, Narina S, Pruett-Miller SM, Peng J, Rankovic Z and Green DR: Ca^{2+}-mediated mitochondrial inner membrane permeabilization induces cell death independently of Bax and Bak. Cell Death Differ 29: 1318-1334, 2022.
30. Tang Q, Jin M, Xiang J, Dong M, Sun H, Lau C and Li G: The membrane permeable calcium chelator BAPTA-AM directly blocks human ether a-go-go-related gene potassium channels stably expressed in HEK 293 cells. Biochem Pharmacol 74: 1596-1607, 2007.
31. Fu Z, Fan Q, Zhou Y, Zhao Y and He Z: Elimination of intracellular calcium overload by BAPTA-AM-loaded liposomes: A promising therapeutic agent for acute liver failure. ACS Appl Mater Interfaces 11: 39574-39585, 2019.
32. He Z, Tang H, You X, Huang K, Dhinakar A, Kang Y, Yu Q and Wu J: BAPTA-AM nanoparticle for the curing of acute kidney injury induced by ischemia/reperfusion. J Biomed Nanotechnol 14: 868-883, 2018.
33. Hong X, Wang H, Yang J, Lin B, Min Q, Liang Y, Huang P, Zhong Z, Guo S, Huang B and Xu YF: Systemic injury caused by taurocholate-induced severe acute pancreatitis in rats. Exp Ther Med 24: 468, 2022.
34. Laukkarinen JM, Van Acker GJ, Weiss ER, Steer ML and Perides G: A mouse model of acute biliary pancreatitis induced by retrograde pancreatic duct infusion of Na-taurocholate. Gut 56: 1590-1598, 2007.
35. Aho HJ, Suonpää K, Ahola RA and Nevalainen TJ: Experimental pancreatitis in the rat. Ductal factors in sodium taurocholate-induced acute pancreatitis. Exp Pathol 25: 73, 1984.
36. Lange JF, van Gool J and Tytgat GNJ: Experimental pancreatitis in the rat: Role of bile reflux in sodium taurocholate-induced acute haemorrhagic pancreatitis. Eur Surg Res 18: 369-374, 1986.
37. Tani S, Otsuki M, Itoh H, Nakamura T, Fujii M, Okabayashi Y, Fujisawa T and Baba S: The protective effect of the trypsin inhibitor urinastatin on cerulein-induced acute pancreatitis in rats. Pancreas 3: 471-476, 1988.
38. Wang GP, Wen JM, Wen PM, Wilbur RRM, Zhou SMP and Xiao XP: The effect of Somatostatin, Ulinastatin and Salvia miltiorrhiza on severe acute pancreatitis treatment. Am J Med Sci 346: 371-376, 2013.
39. Sag S, Imamoglu M, Sarihan H, Yulug E, Alver A, Geze Saatci S and Cay A: Effects of carbon dioxide pneumoperitoneum on exocrine and endocrine functions, and oxidative state of rat pancreas. Biotech Histochem 96: 257-262, 2021.
40. Wenhong D, Jia Y, Weixing W, Xiaoyan C, Chen C, Sheng X, Hao J and Huang RS: Zerumbone Attenuates the severity of acute necrotizing pancreatitis and pancreatitis-induced hepatic injury. Mediat Inflamm 2012: 156507-156512, 2012.
41. Otani T and Matsukura A: Premature trypsinogen activation during cerulein pancreatitis in rats occurs inside pancreatic acinar cells. Pancreas 20: 421-422, 2000.
42. Saluja A, Dudeja V, Dawra R and Sah RP: Early Intra-acinar events in pathogenesis of pancreatitis. Gastroenterology 156: 1979-1993, 2019.
43. Mort JS and Buttle DJ: Cathepsin B. Int J Biochem Cell Biol 29: 715-720, 1997.
44. Winer J, Jung CK, Shackel I and Williams PM: Development and validation of real-time quantitative reverse transcriptase-polymerase chain reaction for monitoring gene expression in cardiac myocytes in vitro. Anal Biochem 270: 41-49, 1999.
45. Gerasimenko JV, Gerasimenko OV and Petersen OH: The role of Ca2+ in the pathophysiology of pancreatitis. J Physiol 592: 269-280, 2014.
46. Maléth J and Hegyi P: Ca2+ toxicity and mitochondrial damage in acute pancreatitis: Translational overview. Philos Trans R Soc Lond B Biol Sci 371: 20150425, 2016.
47. Ismail OZ and Bhayana V: Lipase or amylase for the diagnosis of acute pancreatitis? Clin Biochem 50: 1275-1280, 2017.
48. Szatmary P, Grammatikopoulos T, Cai W, Huang W, Mukherjee R, Halloran C, Beyer G and Sutton R: Acute pancreatitis: Diagnosis and treatment. Drugs 82: 1251-1276, 2022.
49. Das D, Mukherjee S, Das AS, Mukherjee M and Mitra C: Aqueous extract of black tea (Camellia sinensis) prevents ethanol+cholecystokinin-induced pancreatitis in a rat model. Life Sci 78: 2194-2203, 2006.
50. Guicciardi ME, Deussing J, Miyoshi H, Bronk SF, Svingen PA, Peters C, Kaufmann SH and Gores GJ: Cathepsin B contributes to TNF-alpha-mediated hepatocyte apoptosis by promoting mitochondrial release of cytochrome c. J Clin Invest 106: 1127-1137, 2000.
51. He R, Wang Z, Dong S, Chen Z and Zhou W: Understanding Necroptosis in pancreatic diseases. Biomolecules 12: 828, 2022.
52. Sendler M, Maertin S, John D, Persike M, Weiss FU, Krüger B, Wartmann T, Wagh P, Halangk W, Schaschke N, *et al*: Cathepsin B activity initiates apoptosis via digestive protease activation in pancreatic acinar cells and experimental pancreatitis. J Biol Chem 291: 14717-14731, 2016.
53. Zhang X, Lin Q and Zhou Y: Progress of study on the relationship between mediators of inflammation and apoptosis in acute pancreatitis. Digest Dis Sci 52: 1199-1205, 2007.
54. Lankisch PG, Apte M and Banks PA: Acute pancreatitis. Lancet 386: 85-96, 2015.
55. Song Y, Zhang Z, Yu Z, Xia G, Wang Y, Wang L, Peng C, Jiang B and Liu S: Wip1 Aggravates the Cerulein-induced cell autophagy and inflammatory injury by targeting STING/TBK1/IRF3 in acute pancreatitis. Inflammation 44: 1175-1183, 2021.
56. Criddle DN, Gerasimenko JV, Baumgartner HK, Jaffar M, Voronina S, Sutton R, Petersen OH and Gerasimenko OV: Calcium signalling and pancreatic cell death: Apoptosis or necrosis? Cell Death Differ 14: 1285-1294, 2007.
57. Zhou X, Chen H, Wei X, He Y, Xu C and Weng Z: Establishment of a mouse severe acute pancreatitis model using retrograde injection of sodium taurocholate into the Biliopancreatic duct. J Vis Exp 182: e63129, 2022.
58. Petersen OH: Ca2+-induced pancreatic cell death: Roles of the endoplasmic reticulum, zymogen granules, lysosomes and endosomes. J Gastroenterol Hepatol 23 (Suppl 1): S31-S36, 2008.
59. Li J, Zhou R, Zhang J and Li Z: Calcium signaling of pancreatic acinar cells in the pathogenesis of pancreatitis. World J Gastroenterol 20: 16146-16152, 2014.
60. Wang Q, Bai L, Luo S, Wang T, Yang F, Xia J, Wang H, Ma K, Liu M, Wu S, *et al*: TMEM16A Ca^{2+}-activated Cl^- channel inhibition ameliorates acute pancreatitis via the IP3R/Ca2+/NFκB/IL-6 signaling pathway. J Adv Res 23: 25-35, 2020.
61. Yan J, Wang Y, Zhang J, Liu X, Yu L and He Z: Rapidly blocking the calcium Overload/ROS production feedback loop to alleviate acute kidney injury via microenvironment-responsive BAPTA-AM/BAC Co-delivery Nanosystem. Small 19: e2206936, 2023.
62. Fanczal J, Pallagi P, Görög M, Diszházi G, Almássy J, Madácsy T, Varga Á, Csernay Biró P, Katona X, Tóth E, *et al*: TRPM2-mediated extracellular Ca^{2+} entry promotes acinar cell necrosis in biliary acute pancreatitis. J Physiol 598: 1253-1270, 2020.
63. Ricardo Carvalho VP, Figueira da Silva J, Buzelin MA, Antônio da Silva Júnior C, Carvalho Dos Santos D, Montijo Diniz D, Binda NS, Borges MH, Senna Guimarães AL, Rita Pereira EM and Gomez MV: Calcium channels blockers toxins attenuate abdominal hyperalgesia and inflammatory response associated with the cerulein-induced acute pancreatitis in rats. Eur J Pharmacol 891: 173672, 2021.
64. Zhang P, Yin X, Wang X, Wang J, Na G and Ирина Павловна K: Paeonol protects against acute pancreatitis by Nrf2 and NF-κB pathways in mice. J Pharm Pharmacol 74: 1618-1628, 2022.
65. Mayerle J, Sendler M, Hegyi E, Beyer G, Lerch MM and Sahin-Tóth M: Genetics, cell biology, and pathophysiology of pancreatitis. Gastroenterology 156: 1951-1968, 2019.
66. Werneburg NW, Guicciardi ME, Bronk SF and Gores GJ: Tumor necrosis factor-alpha-associated lysosomal permeabilization is cathepsin B dependent. Am J Physiol Gastrointest Liver Physiol 283: G947-G956, 2002.

67. Forsmark CE, Swaroop Vege S, Wilcox CM and Campion EW: Acute pancreatitis. N Engl J Med 375: 1972-1981, 2016.
68. Hines OJ and Pandol SJ: Management of severe acute pancreatitis. BMJ 367: l6227, 2019.
69. Li L, Tucker RW, Hennings H and Yuspa SH: Chelation of intracellular Ca2+ inhibits murine keratinocyte differentiation in vitro. J Cell Physiol 163: 105-114, 1995.
70. Tymianski M, Spigelman I, Zhang L, Carlen PL, Tator CH, Charlton MP and Wallace MC: Mechanism of action and persistence of Neuroprotection by Cell-permeant Ca2+ chelators. J Cereb Blood Flow Metab 14: 911-923, 1994.
71. Toronyi É, Hamar J, Perner F and Szende B: Prevention of apoptosis reperfusion renal injury by calcium channel blockers. Exp Toxicol Pathol 51: 209-212, 1999.
72. Jang M, Shin M, Cho Y, Baik H, Kim S, Hwang E and Kim C: 1,2-bis (2-aminophenoxy)ethane-N,N,N'N'-tetraacetic acid (BAPTA-AM) inhibits caffeine-induced apoptosis in human neuroblastoma cells. Neurosci Lett 358: 189-192, 2004.
73. Hsu S, Jan C and Liang W: The investigation of the pyrethroid insecticide lambda-cyhalothrin (LCT)-affected Ca^{2+} homeostasis and -activated $Ca2^{+}$-associated mitochondrial apoptotic pathway in normal human astrocytes: The evaluation of protective effects of BAPTA-AM (a selective Ca^{2+} chelator). Neurotoxicology 69: 97-107, 2018.
74. Frosali S, Leonini A, Ettorre A, Di Maio G, Nuti S, Tavarini S, Di Simplicio P and Di Stefano A: Role of intracellular calcium and S-glutathionylation in cell death induced by a mixture of isothiazolinones in HL60 cells. Biochim Biophys Acta 1793: 572-583, 2009.
75. Nathens AB, Curtis JR, Beale RJ, Cook DJ, Moreno RP, Romand J, Skerrett SJ, Stapleton RD, Ware LB and Waldmann CS: Management of the critically ill patient with severe acute pancreatitis. Crit Care Med 32: 2524-2536, 2004.
76. Maher MM, Lucey BC, Gervais DA and Mueller PR: Acute pancreatitis: The role of imaging and interventional radiology. Cardiovasc Inter Rad 27: 208-225, 2004.
77. Nordestgaard AG, Wilson SE and Williams RA: Correlation of serum amylase levels with pancreatic pathology and pancreatitis etiology. Pancreas 3: 159-161, 1988.
78. Moridani MY and Bromberg IL: Lipase and pancreatic amylase versus total amylase as biomarkers of pancreatitis: An analytical investigation. Clin Biochem 36: 31-33, 2003.
79. Song R, Yu D and Park J: Changes in gene expression of tumor necrosis factor alpha and interleukin 6 in a canine model of caerulein-induced pancreatitis. Can J Vet Res 80: 236-241, 2016.
80. Jiang CY, Wang W, Tang JX and Yuan ZR: The adipocytokine resistin stimulates the production of proinflammatory cytokines TNF-α and IL-6 in pancreatic acinar cells via NF-κB activation. J Endocrinol Invest 36: 986-992, 2013.
81. Fang S, Li P, Zhu C, Han X, Bao P and Guo W: Research progress of ulinastatin in the treatment of liver diseases. Int J Clin Exp Patho 13: 2720-2726, 2020.

Copyright © 2024 Fu et al. This work is licensed under a Creative Commons Attribution-NonCommercial-NoDerivatives 4.0 International (CC BY-NC-ND 4.0) License.